Development of a position-sensitive fast scintillator ($LaBr_3$(Ce)) detector setup for gamma-ray imaging application

Biswajit Das, R. Palit, R. Donthi, A. Kundu, Md. S. R. Laskar, P. Dey, D. Negi, F. S. Babra, S. Jadhav, B. S. Naidu, and A. T. Vazhappilly

Department of Nuclear and Atomic Physics,
Tata Institute of Fundamental Research, Mumbai - 400 005, India
Corresponding author: biswajit.das@tifr.res.in

***Abstract*—We have characterized a Cerium doped Lanthanum Bromide ($LaBr_3$(Ce)) crystal coupled with the position-sensitive photo-multiplier system for the gamma-ray imaging application. One can use this detector set-up for the scanning of high purity germanium detectors for pulse shape analysis in gamma-ray spectroscopy experiments and the image formation of an object by Compton back-scattering . The sensor has been tested for energy, timing and position information of the gamma-rays interacting within the detector crystal. The GEANT4 simulation results are consistent with the experimental results. We have reconstructed the image of irradiation spots in different positions throughout the detector crystal. Position resolution is found to be around 3.5 mm with the 2 mm collimated gamma-rays. The 2-d image of hexagonal Bismuth Germanate (BGO) crystal and a cylindrical $LaBr_3$(Ce) crystal have been reconstructed in coincidence technique. The performance of the detector for imaging application has been investigated by coincidence technique in GEANT4 simulation and compared with the experimental data. We have reconstructed the 2-d images of objects with various geometrical shapes by Compton back-scattered events of the gamma-rays. This position-sensitive detector can be used as an absorber of a Compton camera for the image reconstruction of an extended radioactive source. One can also use this kind of set-up as in radiation imaging and many other applications where the energy and source position of the gamma-ray is the main interest.**

***Keywords* —γ-ray instrument; $LaBr_3$ (Ce) crystal coupled with PSPMT; γ-ray imaging**

I. Introduction

Position Sensitive Photo Multiplier Tube (PSPMT) coupled with scintillator crystal converts the associated scintillation light into a current signal in the localized photo-cathode [1, 2]. The current signal distribution contains important information regarding energy, timing and the interaction position of the gamma-ray in the detector crystal [3, 4, 5]. Such position measurements are also often carried out using other detector arrays by combining signal channels in a multichannel analog readout, or by using complex segmented detectors, but potentially, at the expense of other performance parameters, and also not viable in compact arrangements. In the present work, a Ce doped $LaBr_3$ crystal coupled with a position sensitive photo-multiplier assembly has been characterized, where the signal processing unit could be made highly compact by coupling a resistive chain with the PMT. In this way, the electronics for signal processing can be reduced without impacting the image quality [4]. There are some work on position characterization of the similar kind of detector where individual readout has been read and digitized[6, 7]. This setup has a versatile impact, either as a stand-alone assembly or in concurrence with an ancillary detector in various important fields. It is expected to find use in i) scanning of segmented high purity Ge (HPGe) detectors for pulse shape analysis [8-11] in gamma-ray spectroscopy experiments, in order to reconstruct the interaction path within the detector volume, ii) testing the electrical response of granular Si charged-particle detectors/sensors as a function of the interaction position of incident particle [12], iii) medical imaging of large organs/sections of the body, for situations where conventional cameras may be difficult to optimize, iv) small animal imaging for pre-clinical research in the pharmaceutical sector, v) the defense and nuclear waste-disposal sectors for identification of radiation sources as well as for environmental radiation surveys by means of a scatterer-absorber configuration.

In this work, a $LaBr_3$(Ce) scintillator crystal, with high light output, low self-absorption, and high sensitivity [13, 14] for low energy gamma-rays, has been coupled with a compact readout PSPMT and employed for gamma-ray imaging. This detector has an energy resolution value of about 6% for 511 keV gamma-ray photo peak. The signal produced in the photomultiplier tube by scintillation light output of the crystal has been distributed through a resistive chain circuit. The front, side, and back view of the detector assembly are shown in Fig. 1. The scintillator crystal is chosen on account of its good timing resolution, in order to reject the scattered and background events by coincidence technique for image reconstruction [15]. Spots at different positions on the PSPMT-coupled-crystal have been irradiated, and the position resolution has been determined therefrom. Subsequently, the 2-d images of auxiliary detectors, such as a hexagonal-shaped BGO crystal as well as a cylindrical $LaBr_3$(Ce) crystal, have been reconstructed in the PSPMT detector using the coincidence technique. The experimental results are found to be in good agreement with simulations carried out using the GEANT4 architecture (version 4.10.05). Subsequently, the

applicability of the present system for imaging via the Compton back-scattering technique has been illustrated by simulating the 2-d image of a ring-shaped scatterer. Further more, this kind of setup can be use as a Compton's camera by adding a thin position sensitive detector as scatterer with this $LaBr_3$(Ce)-PSPMT detector.

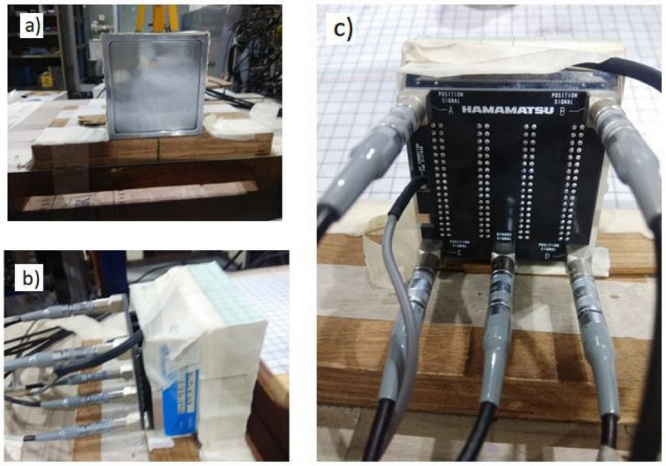

Fig. 1. $LaBr_3$(Ce)-PSPMT detector coupled with resistive network: a) Front; b) Side; c) Back views, showing four anode (position) signals at four corners along with the cathode signal (lower middle).

II. Materials and Detector Details

The position sensitive detector crystal used in this work has been manufactured using pure $LaBr_3$ with 5% doping of Ce. The crystal was grown by Saint Gobain Crystals and Detectors [16]. It has a high density (5.08 gm/cm 3), high light output of ≈ 63 photons/keV, and a fast timing characteristics with time resolution less than 500 ps. ^{138}La (natural abundance 0.089%) is known to decay by two parallel paths, namely (i) β^- decay to ^{138}Ce (34.4%) and (ii) electron capture decay to ^{138}Ba (65.6%) [17]. These processes are associated with the emission of 789 keV and 1436 keV γ-transitions [18], respectively, which also contribute to the total internal activity of the detector material, measured to be ∼ 3 counts sec^{-1} cm^{-3} in the present work. An appropriate thickness of the crystal is chosen that allows seamless detection for a few hundred keV gamma-rays, without much contamination owing to internal activity. The crystal has dimensions measuring 5.08 cm × 5.08 cm × 0.6 cm , and has been coupled to a compact readout PSPMT (Hamamatsu-8500C) [19] through a 5 mm long light guide. The entire assembly is housed inside a 0.5 mm thick aluminium casing. The PSPMT of demountable design is equipped with a mesh of 8 horizontal (X) and 8 vertical (Y) anode-wires, as well as a bi-alkali photo-cathode. The output signal from the photo-cathode is distributed among the anode mesh-wires through an external network of resistors, from which four position signals are derived by means of charge-dividing detection. This allows a compact setup with nominal electronic circuitry.

III. Experimental Details

The cathode signal of the $LaBr_3$(Ce)-PSPMT gives the gamma-ray energy and timing information, and the four anode signals contain X-Y position information of the gamma-ray interaction point in the detector crystal. An operating voltage of -1050 V leads to low internal noise and high signal gain. For characterization of the position sensitive detector, such as estimation of spatial resolution of irradiation spots, as well as for position calibration of the crystal, a ^{57}Co (0.5 μCi) radioactive source (122 keV gamma-ray) [5] has been used. In the course of data acquisition, the performance of the crystal as an imaging detector has been investigated, wherein the events due to internal radioactivity and scattering within the crystal have been suppressed as a result of acquiring data in coincidence mode. In this regard, a ^{22}Na (14 μCi) radioactive source has been used where positron-electron annihilation leads to simultaneous emission of two 511 keV gamma-rays in the diametrically opposite directions [20]. The schematic diagram of the set-up for the coincidence technique used in this work is shown in Fig. 2.

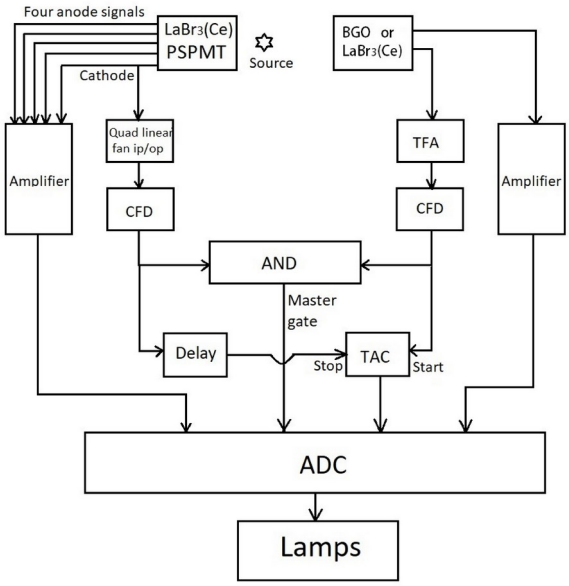

Fig. 2. Schematic diagram of the coincidence set-up, where a hexagonal BGO/ cylindrical $LaBr_3$(Ce) is chosen as the complementary detector along with the position sensitive detector under investigation.

To detect these two 511 keV gamma-rays, the $LaBr_3$(Ce)-PSPMT is used along with an auxiliary detector kept on the opposite side of the radioactive source. The distance of the source from both the detectors, placed face-to-face, has been optimized for count rate handling capacity of the data acquisition system and also to obtain an optimum size of the image of the complementary detector reconstructed by the $LaBr_3$(Ce)-PSPMT. For this purpose, a hexagonal BGO detector and a cylindrical $LaBr_3$(Ce) detector have been used as auxiliary detectors, with dimensions of 5.59 cm × 7.62 cm (height × length) and 5.08 cm × 5.08 cm (diameter × length) respectively. Only those yields recorded by the $LaBr_3$(Ce)-PSPMT assembly have been registered as true events which were in coincidence with the BGO/cylindrical $LaBr_3$(Ce) detector.

All current approaches to the characterization of the

position sensitive detector are based on the standard CAMAC acquisition system. To extract energy and position information, the cathode and four anode signals of the $LaBr_3$(Ce)-PSPMT, respectively, have been processed using spectroscopic amplifiers. The coincidence interval is defined using a TAC module, wherein the signal of the complementary BGO/cylindrical $LaBr_3$(Ce) detector, after being processed through a Constant Fraction Discriminator (CFD) module, triggers/starts the coincidence event while the corresponding CFD output of $LaBr_3$(Ce)-PSPMT cathode terminates the window. The common timing reference window for the registered events, i.e. the master gate, has been generated by the AND output of the two aforementioned CFD signals, in order to control the trigger rate of the data acquisition system. A typical time profile of the raw energy signal and position signal are shown in Fig. 3 . Only those events have been accepted during acquisition wherein the four anode signals as well as the TAC output remain well within this window. The analog pulses have been digitized using 8-channel 12-bit ADC. The Linux Advanced Multi-Parameter System (LAMPS) [21, 22] package has been used for the data acquisition system and further analysis has been performed by employing the ROOT package [23].

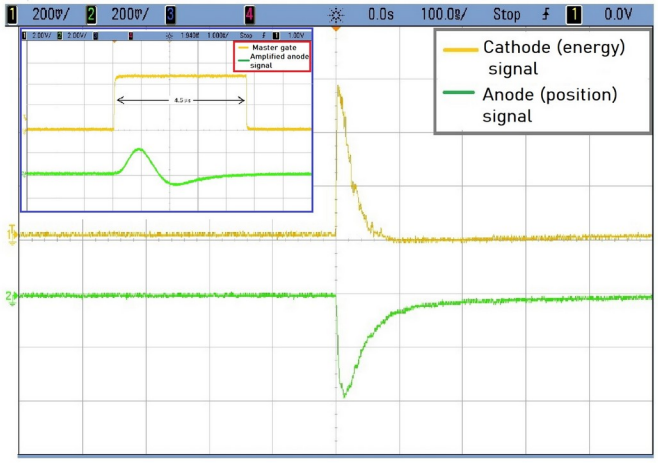

Fig. 3. Typical raw energy signal (from cathode) and position signal (anode). Inset: One of the anode (position) signals (bottom) as seen with respect to the reference master gate window (top).

IV. Analysis and Results

A. Energy and time resolution

The gamma-ray energy spectrum of the $LaBr_3$(Ce)-PSPMT detector has been calibrated using standardized ^{22}Na, ^{54}Mn, ^{57}Co, ^{133}Ba, ^{137}Cs, and ^{152}Eu radioactive sources. Energy resolutions of ~9.5% for 122 keV and ~6% for 511 keV (Fig. 4(a)) have been measured, in good agreement with GEANT4 simulations. In coincidence with the auxiliary cylindrical $LaBr_3$(Ce) crystal, timing resolution of 761(2) ps has been obtained from the TAC spectrum generated between the auxiliary detector and the position sensitive detector, as shown in Fig. 4(b).

B. Position resolution

Nine different spots were selectively irradiated on the $LaBr_3$ (Ce)-PSPMT detector with 122 keV gamma-ray source, collimated using a perforated (2 mm) lead block of 20 mm thickness.

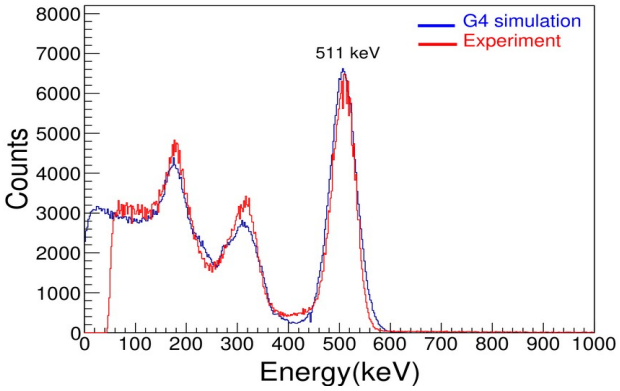

4(a)

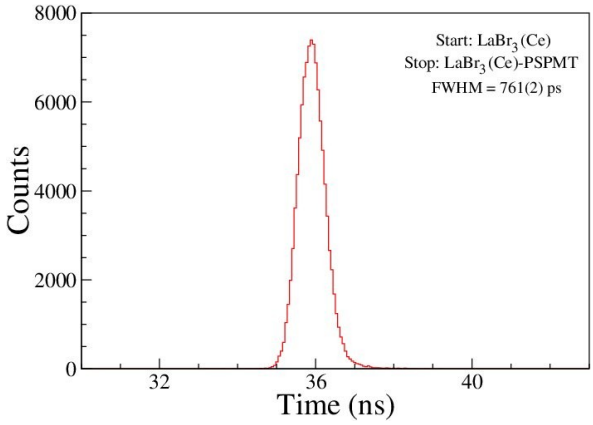

4(b)

Fig. 4. a) Simulated and experimental gamma-ray energy spectra of ^{22}Na source for the $LaBr_3$Ce)-PSPMT detector obtained in coincidence with 511 keV γ-energy in the BGO spectrum. The calculated energy resolution of the 511 keV photo-peak is ~6%. b) TAC spectrum, with the timing from the auxiliary cylindrical $LaBr_3$(Ce) taken as the START signal, and that from the position sensitive detector as the STOP signal.

The arrangement is represented in Fig. 5 . The resultant amplitudes of the four anode signals corresponding to each irradiated spot depend on the voltage drop through the resistive network, and the interaction points (X-position and Y-position) of the incident gamma-rays on the detector crystal have subsequently been determined as follows [3]:

$$X_{position} = \frac{(a_2 B + a_4 D)}{(A+B+C+D)} + b$$

$$Y_{position} = \frac{(a_3 C + a_4 D)}{(A+B+C+D)} + b$$

where, A, B, C and D are the amplitudes of the four anode

signals, a_1 , a_2 , a_3 and a_4 are the gain factors of the amplifiers (adjusted to be identical in the present measurement), with b as a manually-defined offset factor for the position spectra. The spectrum of the nine irradiated spots has been generated with an energy gate on 122 keV gamma-rays recorded from $LaBr_3$ (Ce)-PSPMT cathode, and the X- and Y-positions of the interaction points have been obtained therefrom.

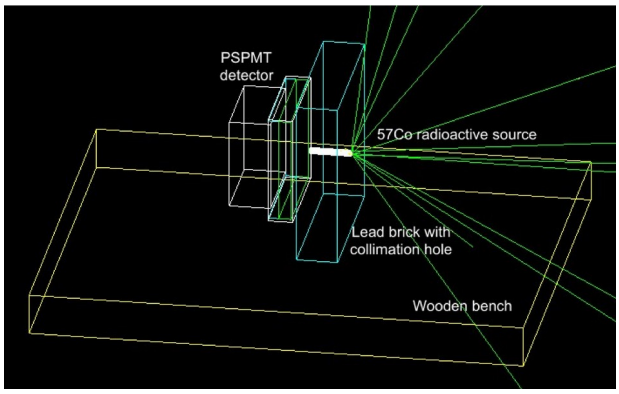

Fig. 5. Geometry of GEANT4 simulation for crystal calibration with lead brick collimator with ^{57}Co source.

The observed spectrum has also been validated by means of GEANT4 simulation, taking all possible physics processes into account. gamma-ray photons, electrons and positrons are expected to be produced during the interaction of the incident gamma-rays. The considered interaction mechanisms for the γ-photons are photoelectric effect, Compton scattering, and pair production. The electrons and positrons so produced can undergo multiple scatterings, ionizations and emit Bremsstrahlung radiation, while in addition, the positron can also undergo annihilation. The image has been reconstructed using those points at which maximum energy is deposited by the electrons generated along the interaction path of the incident gamma-rays in the crystal volume. The FWHM for each spot is ≈ 3.5 mm in the simulated spectrum (Fig. 6(a)), while the measured FWHM for the different spots lies in the range of about 3.5-4.0 mm (Fig. 6(b)). Since the measured spectrum is susceptible to electronic noise, a slight degradation is seen compared to the simulated outcome.

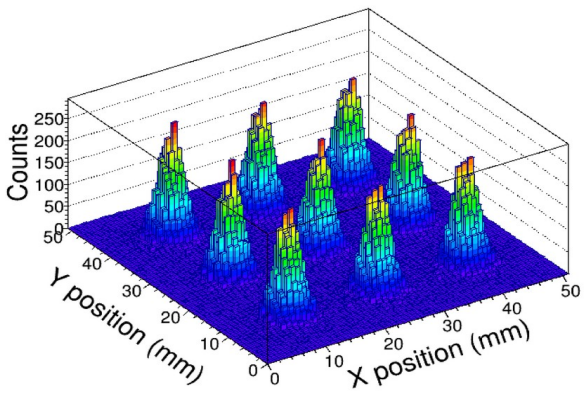

6(a)

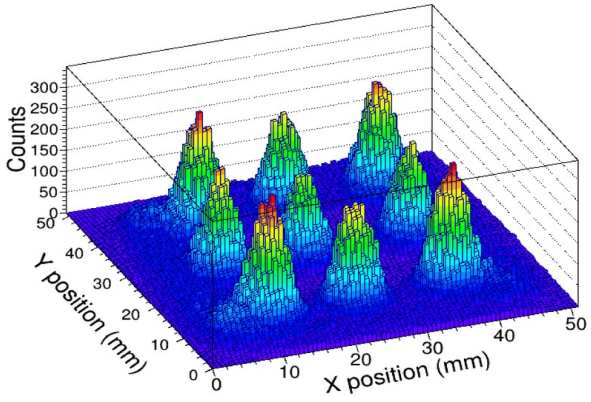

6(b)

Fig. 6: a) GEANT4 simulated and b) experimental result of nine irradiation spots with 2 mm collimated 122 keV gamma-rays on the $LaBr_3$(Ce)-PSPMT crystal.

C. Performance as an imaging detector

The images of a hexagonal BGO detector and a cylindrical $LaBr_3$(Ce) crystal have been generated using the position sensitive detector in a coincidence setup, as illustrated in Fig. 7 for the BGO detector, with energy gate on 511 keV gamma-ray photo-peak of both the detectors.

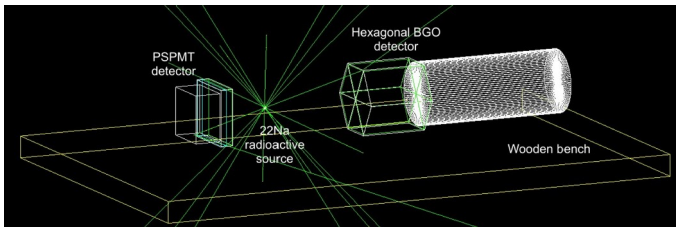

Fig. 7: Geometry of GEANT4 simulation of coincidence set-up of hexagonal BGO and $LaBr_3$(Ce)-PSPMT detectors.

The results compared with simulations are found to be in reasonable agreement in either case. The typical imaging performance is illustrated in Fig. 8. The position resolution, measured from the fit of the 1-d Y-projection of a slice of X-axis (22.5-27.5 mm) of the BGO image (Fig. 9), is 3.77(08) mm.

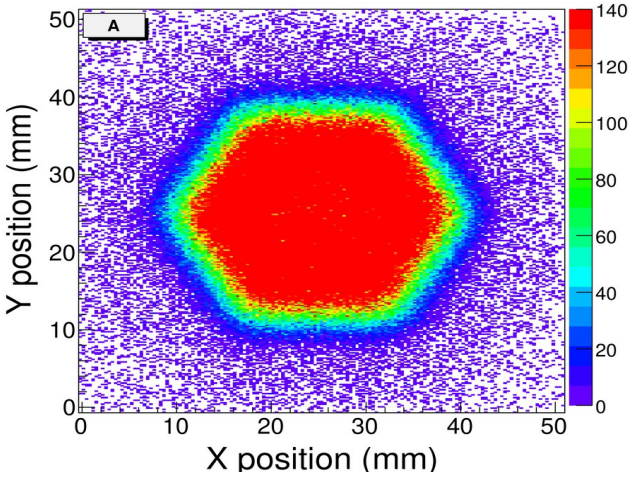

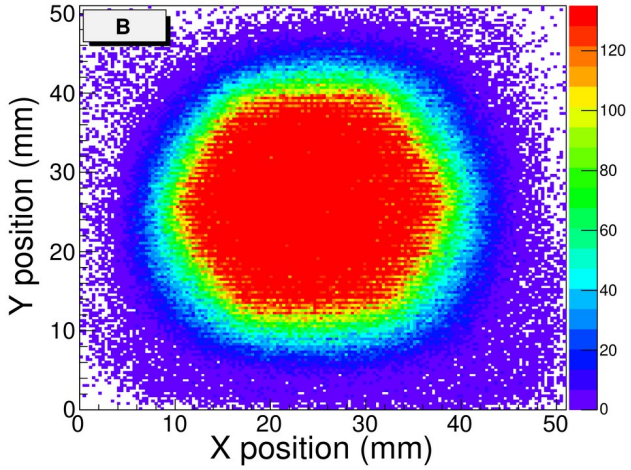

Fig. 8: Simulated (A) and experimental (B) 2-d images of a hexagonal BGO detector reconstructed with the $LaBr_3$(Ce)-PSPMT, in coincidence mode with energy-gating on the 511 keV photo-peak in both detectors.

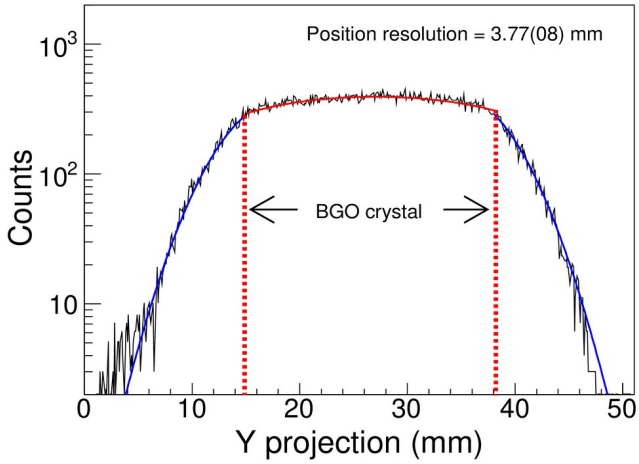

Fig. 9: Y-projection of a slice (X = 22.5 to 27.5 mm) of the experimentally reconstructed BGO image in figure 8(B) showing the variation of the absorbed gamma-ray counts throughout the BGO crystal.

An optimum geometry for image reconstruction by back-scattering technique has been investigated in the GEANT4 framework using the position sensitive $LaBr_3$(Ce) detector in coincidence with a BGO detector as shown in Fig. 10. A steel ring having inner and outer diameter of 3.6 cm and 5.6 cm respectively with 1.1 cm thickness has been used as a scatterer for the incident photons. The position of the lead brick, scatterer, radioactive source, and detectors are chosen in such, so that the ancillary detector can't see the source directly. The lead brick having appropriate thickness to block the gamma-ray directly coming from the source.

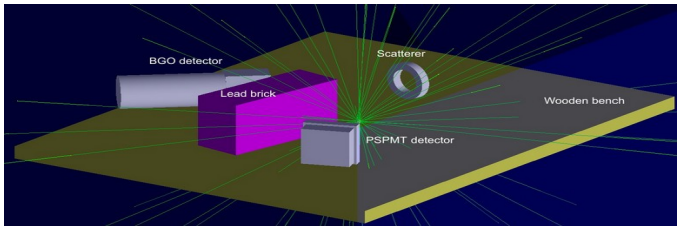

Fig. 10: GEANT4 Geometry of coincidence set-up of BGO and $LaBr_3$(Ce)-PSPMT detectors with a scatterer for Compton back-scattering imaging.

The 150 keV - 230 keV of the gamma-rays recorded in the BGO detector correspond to the back-scattering events from the ring-shaped scatterer. We have reconstructed the image of the ring as shown in Fig. 11, in the simulation with the energy gating condition: 490 keV < E_{PSPMT} <530 keV in the position sensitive $LaBr_3$(Ce) detector and 150 keV < E_{BGO} < 250 keV in the BGO detector. In future, we are planing to do this back-scattering experiment to verify the simulated result as well as to investigate some applications of back-scattering technique.

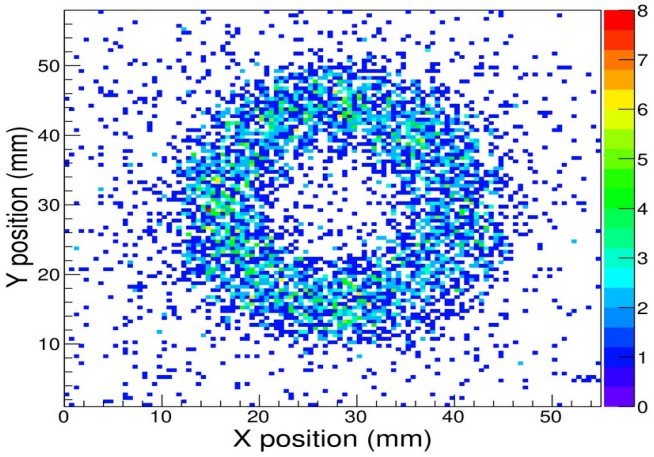

Fig. 11: GEANT4 simulated image of the scatterer (ring) in position sensitive detector with energy gated condition: 490 keV < $E_{LaBr3(Ce)-PSPMT}$ < 530 keV and 150 keV < E_{BGO} < 250 keV.

V. Summary and Conclusions

A $LaBr_3$(Ce)-PSPMT detector setup is developed for gamma-ray tracking and imaging applications. The energy and time characterization of the detector has been studied. A spatial resolution of about 3.5 mm has been obtained with a 2 mm collimated source. GEANT4 simulation for this detector reproduces the measured energy response of the detector and the spatial resolution. The reflection of the scintillation light from the periphery of the detector slightly hampers the position resolution. Sharp 2-d images of a hexagonal shaped BGO and a cylindrical $LaBr_3$(Ce) crystals have been reconstructed using this position-sensitive detector setup, by employing data acquisition in coincidence mode. The 2-d image of a ring shaped scatterer has been reconstructed in GEANT4 by Compton back-scattering technique of the gamma-rays. This setup is expected to find applications in the fields of nuclear and high energy physics for scanning of detectors, as well as for the purpose of imaging in the medical and defense sectors.

Acknowledgment

This work is supported by the Department of Atomic Energy, Government of India, under project No. 12P-R&D-TFR-5.02-0400.

References

[1] S. Majewski, F. Farzanpay, A. Goode, B. Kross, D. Steinbach, A. Weisenberger, M. Williams, and R. Wojcik, (1998) Nuclear Instruments and Methods in Physics Research Section A **409** 520–523

[2] N. Tamda, A. Bakkali, H. Boulahdour, M. Parmentier, A. Pousse, B. Kastler, and J Chavanelle, (2006) Nuclear Instruments and Methods in Physics Research Section A **557** 537 – 543.
[3] A. Banerjee, S. Mandal, P. Roy, S. Mukhopadhyay, G. Mukherjee, M. Kumar, A. Jhingan, and R. Palit, (2019) Nuclear Instruments and Methods in Physics Research Section A **930** 100 – 104.
[4] V. Popov, (2019) Journal of Instrumentation (JINST) **6 C01061**
[5] P. D. Olcott, J. A. Talcott, C. S. Levin, F. Habte, and A. M. K. Foudray, (2005) IEEE Transactions on Nuclear Science **52** 21–27
[6] R. Pani, R. Pellegrini, M.N. Cinti, P. Bennati, M. Betti, F. Vittorini, M. Mattioli, G. Trotta, V. Orsolini Cencelli, R. Scaf, L. Montani, F. Navarria, D. Bollini, G. Baldazzi, G. Moschini, P. Rossi, F. de Notaristefani, Nuclear Instruments and Methods in Physics Research A **572** (2007) 268–269
[7] A. Fabbri,V. Orsolini Cencelli, P. Bennati, M. Nerina Cinti, R. Pellegrini, G. De Vincentis and R. Pani, 2013 JINST **8 C02022**.
[8] M. K. Nguyen, T. T. Truong, M. Morvidone, and Zaidi, International journal of biomedical imaging, Artical id **913893** (2011).
[9] A. Olariu, Member, IEEE, P. Désesquelles, Ch. Diarra, P. Médina, C. Parisel, and C. Santos On behalf of the AGATA Collaboration, IEEE Transactions on nuclear science, VOL. 53, NO. 3, JUNE 2006.
[10] B. Bruyneel, B. Birkenbach, and P. Reiter, The European Physical Journal A **52** (2016) 70.
[11] I. Kojouharov, S. Tashenov, T. Engert, J. Gerl, and H. Schaffner, IEEE Nuclear Science Symposium Conference Record **N46-7** (2007).
[12] B. Alpat and G. Esposito (2003) AIP Conference Proceedings **674** 283.
[13] F. Quarati, A. Bos, S. Brandenburg, C. Dathy, P. Dorenbos, S. Kraft, R. Ostendorf, V. Ouspenski, and A. Owens, Nuclear Instruments and Methods in Physics Research Section A **574** (2007) 115 – 120.
[14] N. Cherepy, S. Payne, S. Asztalos, G. Hull, J. Kuntz, T. Niedermayr, S. Pimputkar, J. Roberts, R. Sanner, T. Tillotson, E. van Loef, C. Wilson, K. Shah, U. Roy, R. Hawrami, A. Burger, L. Boatner, W.-S. Choong, W. Moses, Nuclear Science, IEEE Transactions on **56** (2009) 873 – 880.
[15] A. Kuhn, S. Surti, K. S. Shah, J. S. Karp, in: IEEE Nuclear Science Symposium Conference Record, 2005, volume 4, pp. 5 pp.–2026.
[16] URL http://www.detectors.saint-gobain.com
[17] NNDC URL https://www.nndc.bnl.gov/nudat2/chartNuc.jsp
[18] A. Sonzogni (2003) Nuclear Data Sheets **98** 515 – 664.
[19] Valentino, Francesco and DAbramo E (2007) Nuclear Instruments and Methods in Physics Research Section A **571** 389 – 391.
[20] Robert J.de Meijer, R. Lindsay, M. Tijs, Steven, and H. Limburg, (2019) Radiation Measurements **121** 77 – 85.
[21] A. Chatterjee, A. Kumar, K.Ramachandran, Proceeding of the DAE Symp. on Nucler Physics **55** (2010).
[22] TIFR homepage URL http://www.tifr.res.in/~pell/lamps.html
[23] Root-CERN homepage URL https://root.cern/